Acta Geod Geophys (2015) 50:321–338
DOI 10.1007/s40328-014-0088-y

"Attribute based Inversion" a tool for reservoir characterization: a case study-Kalol Field, Cambay Basin, India

Surajit Gorain · Prabhakar Thakur

Received: 23 July 2014 / Accepted: 10 November 2014 / Published online: 22 November 2014

Abstract With major oil and gas discoveries diminishing in number, industry is turning its attention to redevelop fields with reservoirs (Res) like silts which have otherwise been accorded lower priority earlier. It has always been a challenge to identify the locales with better Re facies development in un-drilled areas of a field and most often many development wells either go dry or turn out to be poor producers, significantly increasing the cost of production from a given field. Kalol Field, Cambay Basin, India is a several decade old discovery with a significant number of development wells. However, the oil recovery remained hardly around 10 %. Most often, the contributing factor for this low recovery is poor Re facies (tight silts) within the major producing sequences like Kalol IX and Kalol X. Hence identifying areas of better Re facies remained a challenging task before the geo-scientists. To overcome this challenge a workflow has been developed for Re characterization based on an "Attribute based Inversion" technique, in which 3D attribute volume of petrophysical properties are calculated through genetic inversion algorithm using a nonlinear correlation between seismic property and log property. Calculated 3D attribute volume of petrophysical properties are utilized further for Re classification and finally geostatistical modeling is performed for Re modeling. The adopted approach is operative even if the Re is very thin (beyond seismic resolution) and can provide a way to generate 3D attribute volumes of log property from seismic and well log data. This approach is also effective in determining the Re geometry and quality of Re, which may help in planning future drilling locations. The application of the workflow has been illustrated with a case study from Kalol Field, Cambay Basin. The obtained results shows that the proposed approach is effective enough in resolving 2–8 m thick Re within Kalol formation. It gives an idea about the Re quality (good or bad Re) and geometry of the Kalol Reservoir in the field. Volumetric calculation shows that there is still

S. Gorain (✉) · P. Thakur
Prize Petroleum Company Limited, 3rd Floor, UCO Bank Building, Parliament Street, New Delhi 110001, India
e-mail: sgorain@gmail.com

P. Thakur
e-mail: drprabhakart@hpcl.co.in

some potential remaining in the field. Hence suitably placing new wells, it is quite possible to increase the productivity of the field.

Keywords Attribute based Inversion · Reservoir characterization · Reservoir modeling · Genetic inversion · Neural network

1 Introduction

Kalol Field is situated in the Ahmadabad–Mehsana tectonic block of Cambay Basin, India (Fig. 1) (Biswas 1987). The silty-sand layers within Kalol formation, namely K-IX and K-X (Middle–Upper Eocene age; Fig. 2) are the main hydrocarbon bearing reservoirs (Res; Gupta et al. 2006).

Kalol formation consists of a combination of thinly inter-bedded sandstone, siltstone, shale and coal. Re intervals can be categorized regionally and locally into numerous units. The lithology of the Kalol pay sands vary widely from silty sands–shaly silts to silty shale

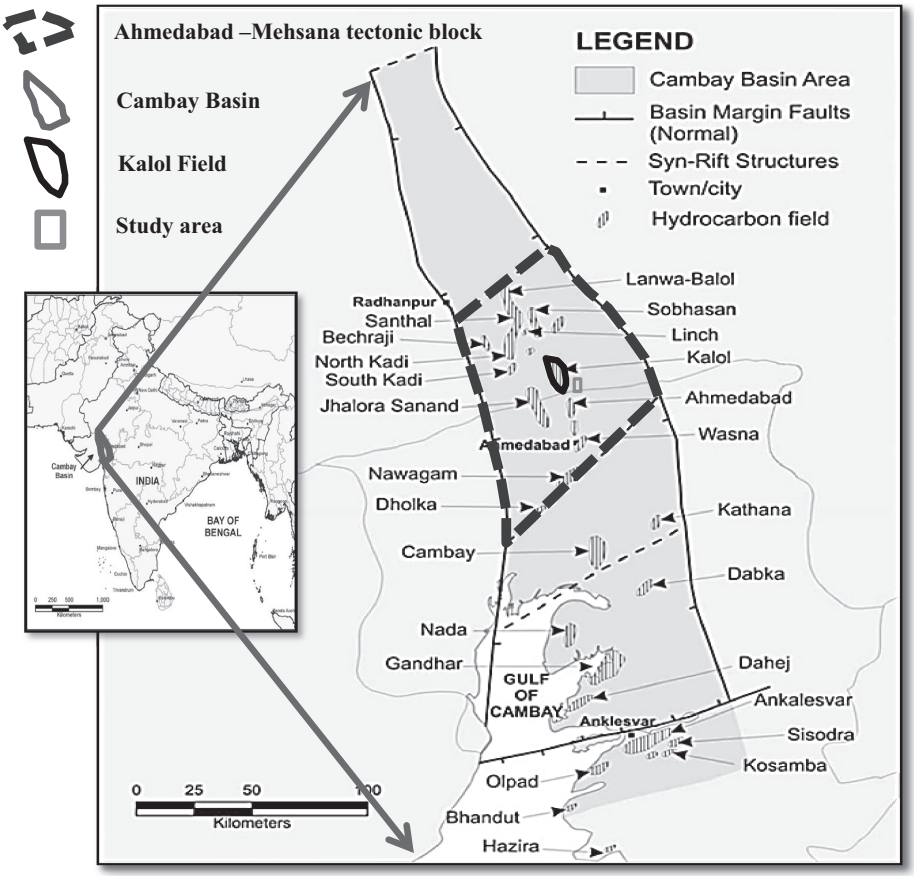

Fig. 1 Location map of the study area (modified from Dhar et al. 1993) showing major hydrocarbon field in Ahmadabad–Mehsana tectonic block. The study area is a part of Kalol Field, Cambay Basin, India

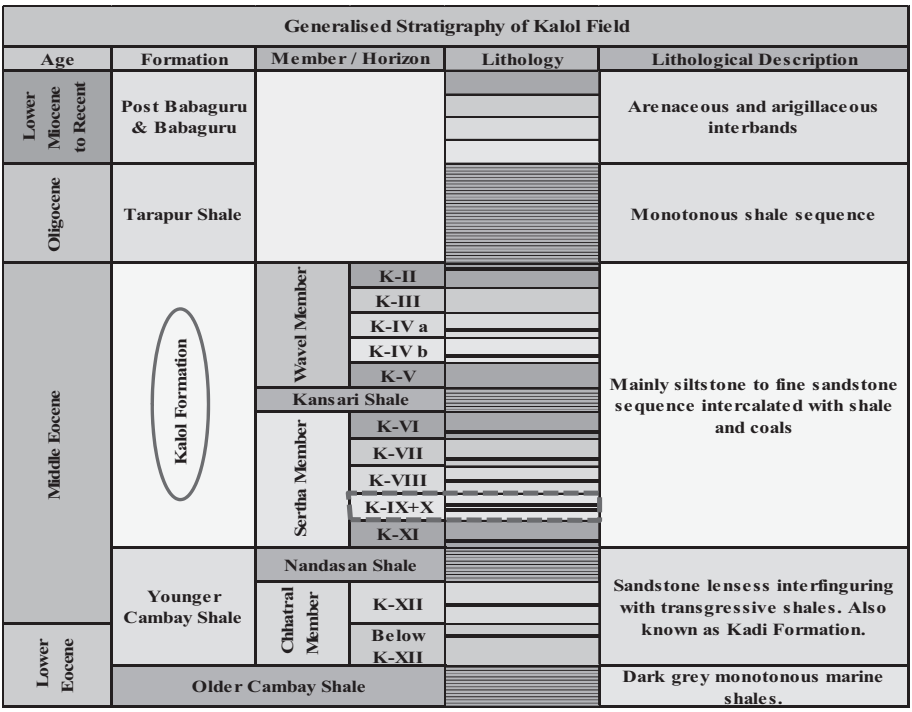

Fig. 2 Generalized stratigraphy of Kalol Field (modified from Jena 2008). The main reservoir lies within the Kalol formation (within K-IX and K-X)

with coal and shale intercalations at places as well as clean porous and permeable siltstones (particularly in K-IX, the main producing horizon; Chatterjee et al. 2006; Gupta et al. 2006).

Kalol pays generally show strati-structural entrapment as the formation represents an Upper Delta Plain depositional system. Hence, the Re quality shows dependency on facies distribution. Figure 2 shows the general stratigraphy of Kalol Field (Jena 2008).

In Kalol Field, a series of thin clastic Res are sandwiched within K-IX and K-X formation. These thin multi-pay sands exhibit several lateral lithological variations (Gupta et al. 2006) and cannot be resolved in the seismic data due to the following reasons:

- The Res are very thin (~2 to ~8 m) and beyond seismic resolution.
- Overlying and underlying coals around the Re, mask the seismic wave leading to lowering in seismic frequency.

Thus, any conventional approach will not be effective in resolving these multi-pay Res. In the present work the conventional seismic inversion have been modified through an integrated approach and an "Attribute based Inversion" (ABI) method has been developed for Re modeling to identify the areas of better Re facies within the productive sequences.

2 Case study

The study area (Fig. 1) is a marginal field of Kalol Field is situated in the Ahmadabad–Mehsana tectonic block of Cambay Basin (Biswas et al. 1993). Like the other parts of the Kalol Field, the main Re lies within Kalol formation, namely K-IX and K-X (Middle–Upper

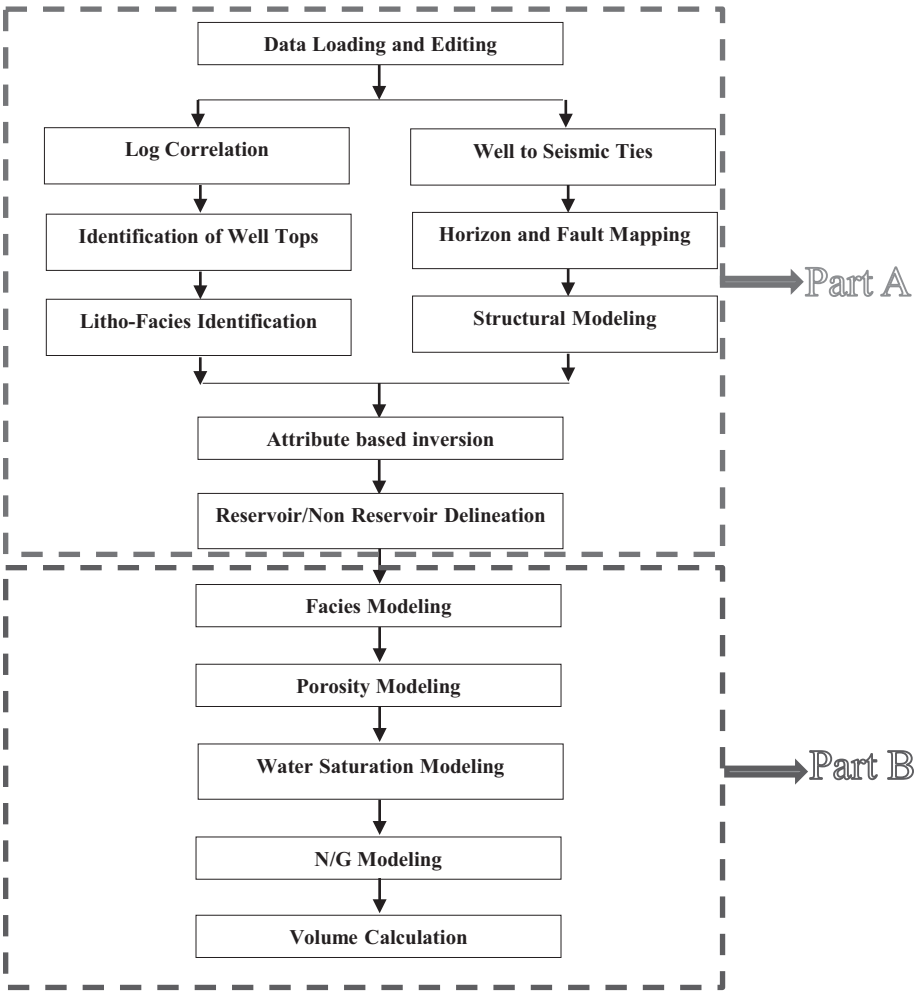

Fig. 3 Workflow of "Attribute based Inversion" and Reservoir Modeling

Eocene age; Fig. 2) and suffers great facies variation. The study area (4.5 sq-km) have full coverage of 3D post stack time migration seismic data with root mean square (RMS) velocity cube and five wells (A–E). Gamma ray (GR) and laterolog-deep-resistivity logs (LLD) are available for all five wells, but interval transit time (DT) and density logs (RHOB) are available only for wells (A–C). In addition, the petrophysical logs viz., porosity (PHI) and water saturation (Sw) logs are also available for all these wells, which are directly used for property modeling. Out of these five wells, only 'Well-A' gives oil production of the order of 10–15 M^3/day whereas other wells produce at very low rates (1–1.5 M^3/day).

3 Methodology and results

The conventional approach has been modified to ABI technique for increasing the resolution to delineate the thin multi-pay zones. The developed workflow for the ABI is shown in Fig. 3. The workflow has two parts

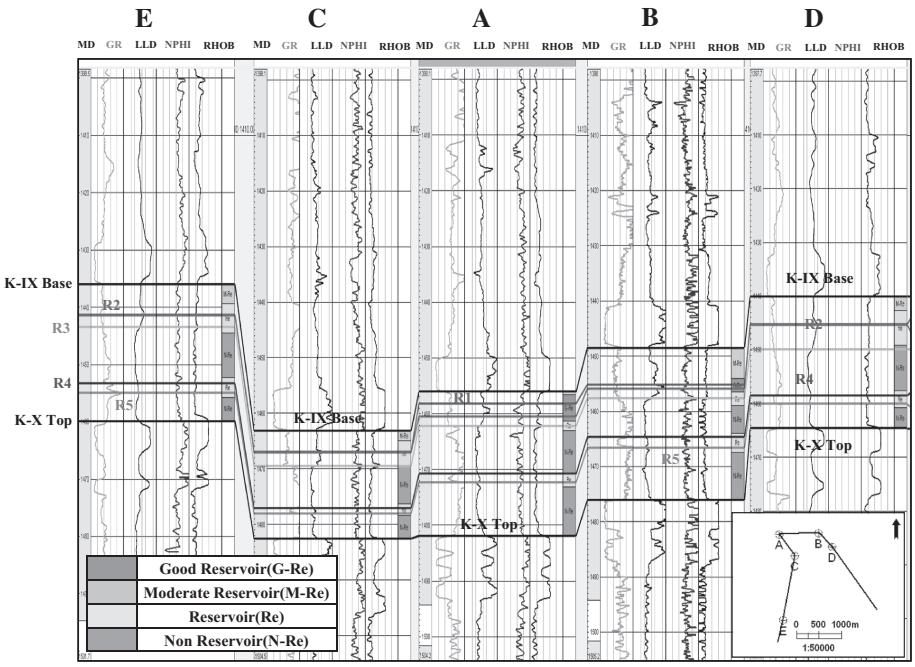

Fig. 4 Well correlation and identified litho-facies log. Litho-facies logs show lateral variation of facies and the reservoirs are very thin

- *Part A* seismo-facies mapping,
- *Part B* Re modeling.

The seismo-facies mapping is the most critical step of ABI and the project is done using Petrel 2011.1 software. The seismo-facies mapping is carried out by using the nonlinear correlation between seismic and log properties. The 3D attribute volume of log property is calculated through genetic algorithm (GA). The calculation of the 3D attribute volume helps in classifying Re and non-Re (N-Re) facies (seismo-facies) volume on a mathematical relation (logical operation). The Re modelling (Part B of the workflow) is used to identify the litho facies variation within the Re. Geo-statistical modeling approach has been used for facies and property modeling taking the seismo facies volume (obtained in Part A of ABI) as a trend volume. We discuss the various steps of ABI with reference to Kalol Field, Cambay Basin, India, in delineating thin multi-pay zones.

3.1 Well correlation and identification of well tops

Based on the available cutting data and basic log character [GR, LLD resistivity, DT, neutron PHI (NPHI) and RHOB] of all five wells, seven well tops (K-IX Base, R1–5 and K-X Top) have been identified. Figure 4 shows the GR, LLD, DT, NPHI and RHOB logs and identified well tops for all the wells. The well correlation map shows that R1 and R2 well tops are present only in Wells A and B and the thickness between them is relatively more at Well A than at Well B.

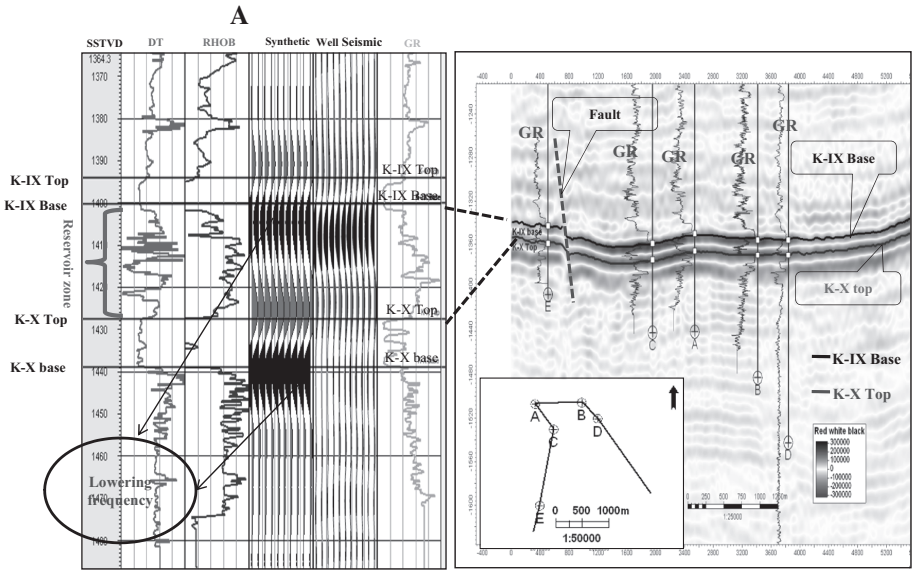

Fig. 5 Synthetic seismogram and QC of well to seismic tie. Overlying and underlying coals masks the seismic wave leading to lowering in seismic frequency and creating resolution problem

3.2 Litho-facies identification

A discrete litho-facies log has been mapped for all the five wells using GR, LLD, DT, NPHI and RHOB and mud logs. The identified four major litho-facies units are good Re (G-Re), moderate Re (M-Re), Re and N-Re (Fig. 4). The litho-facies log suggests that the Re units are have large lateral facies variation.

3.3 Well to seismic tie

Utilizing the available sonic, RHOB and correlated well tops, well-to-seismic tie has been carried out. To quality check (QC) the well-to-seismic-tie, GR logs are overlaid on the arbitrary seismic line passing through the wells and a good correlation is observed. It would have been desirable to carry out synthetic correlation for all the wells but as the sonic log was available for only three wells i.e., A–C, the synthetic correlation has been carried out only for these wells. Figure 5 shows the QC and well-to-seismic tie for the representative Well A only. The correlated well tops are placed in the seismic to map the seismic horizons namely (K-IX Base and K-X Top). As the Re lies within these two mapped horizons, it is difficult to map the Re from seismic because of vertical resolution limit. The synthetic seismogram (Fig. 5) shows that overlying and underlying coals mask the seismic wave leading to lowering in seismic frequency creating resolution problem.

3.4 Horizon and fault mapping

Two horizons namely (K-IX Base and K-X Top) are mapped based on the reflection events in the seismic throughout the 3D volume. The field is less affected by faulting and only one NE–SW trending fault near Well E is visible. Figure 6 shows the mapped horizons and faults.

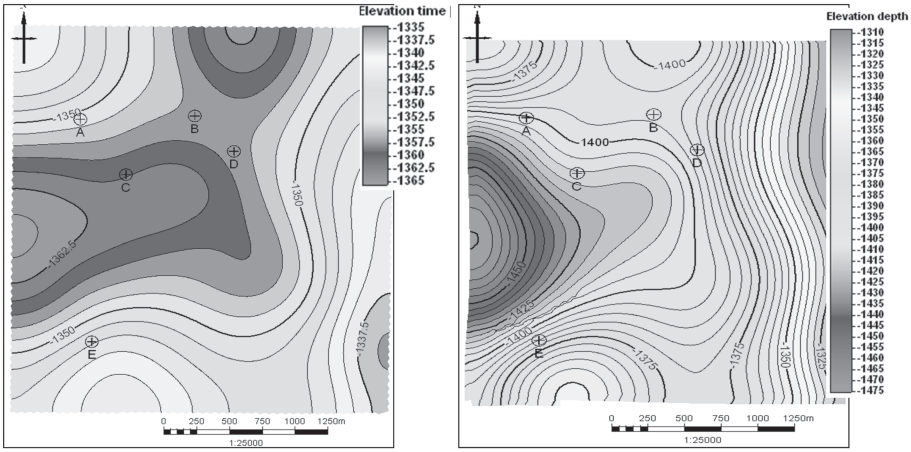

Fig. 6 Time and depth map of K-IX Base level. The time and depth structure maps show that the Well E is structurally shallowest and Well C is the deepest at Kalol Base level

3.5 Structural modeling

Based on the two mapped time horizons (K-IX Base and K-X Top) gridding is done for generating the time structure model. A closely spaced (20 m × 20 m) grid size (equivalent to bin size of the 3D seismic volume) is chosen to accurately sample the Re property for building a representative Re model. The RMS velocity cube and the time–depth (T–D) relationship obtained from synthetic seismogram matching is used to obtain the best-fit velocity model. Time structure map is converted to depth domain using the velocity model. The structure map is generated (Fig. 6) by incorporating the thicknesses of R1–5 as observed at the wells (Fig. 4).

Based on the log signatures, 4 layers between K-IX Base and R1, 3 layers between R1 and R2, 3 layers between R2 and R3, 10 layers between R3 and R4, 2 layers between R4 and R5 and 12 layers between R5 and K-X Tops, respectively are identified and incorporated in the layer cake model. The time and depth structure map of K-IX Base level (Fig. 6) shows that the Well E is structurally shallowest and Well C is the deepest at Kalol level.

3.6 "Attribute based Inversion"

ABI is an approach to derive petro-physical attribute from seismic attribute (amplitude based) and well logs using GA and neural networks (NNs). GA is applied to the learning phase of NN. The use of the genetic learning algorithm allows the Neural Net to find the global minimum of the function and therefore an optimal solution is achieved, while standard Neural Net algorithms generally reach the local minimum error of the function (Veeken et al. 2009).

In general, poststack inversion of seismic data is obtained through model based algorithm. But, here the post stack inversion has been carried out by using GA. Unlike model based algorithms GA does not require an input wavelet or initial model. In addition GA converges faster as compared to model based algorithms.

Genetic inversion (GI) is based on the NN process but with the addition of the GA which together generate a nonlinear multitrace operator. This multitrace operator is produced as a

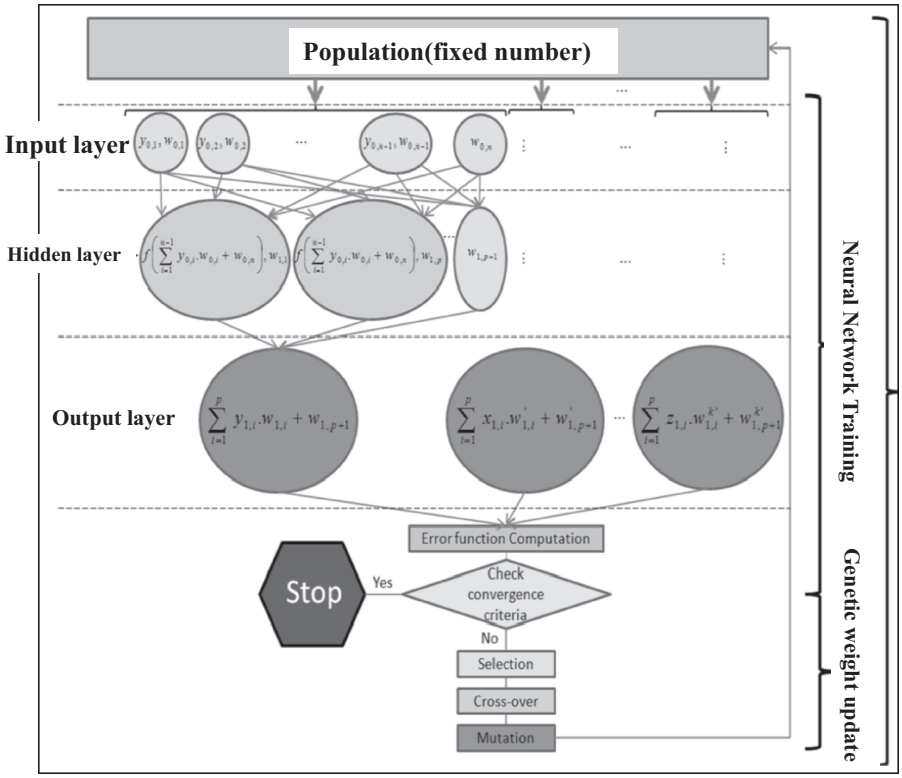

Fig. 7 Genetic inversion workflow scheme (Klinger et al. 2008)

result of training a seismic subvolume against well data. And it is used to invert the seismic data into the desired well log response producing a best fit to the given well data (Veeken et al. 2009). Following, Klinger et al. (2008) the generalized GI workflow scheme is shown in Fig. 7. We have used binary coded GA.

For the sake of completeness we describe GA inversion. The NN is a common multilayer network and uses only one hidden layer in GI. The neural workflow is characterised by the activation (sigmoid) function ($f(x)$), an input/hidden layer ($y_{hidden\,layer}$), bias of the input layer ($w_{0,n}$) and the bias of the hidden layer ($w_{0,p+1}$), respectively (Veeken et al. 2009). The $f(x)$ and $y_{hidden\,layer}$ are represented as:

$$f(x) = \frac{1}{1 + e^{-x}}, \tag{1}$$

and

$$y_{hidden\,layer} = f\left(\sum_{i=1}^{n-1} y_{input,i} \cdot w_{input,i} + w_{input,n}\right). \tag{2}$$

The workflow shows that GA is used in NN training stages to calculate the number of hidden layers to finalized the inversion operator. Once, the inversion operator is finalised the weight of the GA is updated based on the convergence criteria to have the local minimum error.

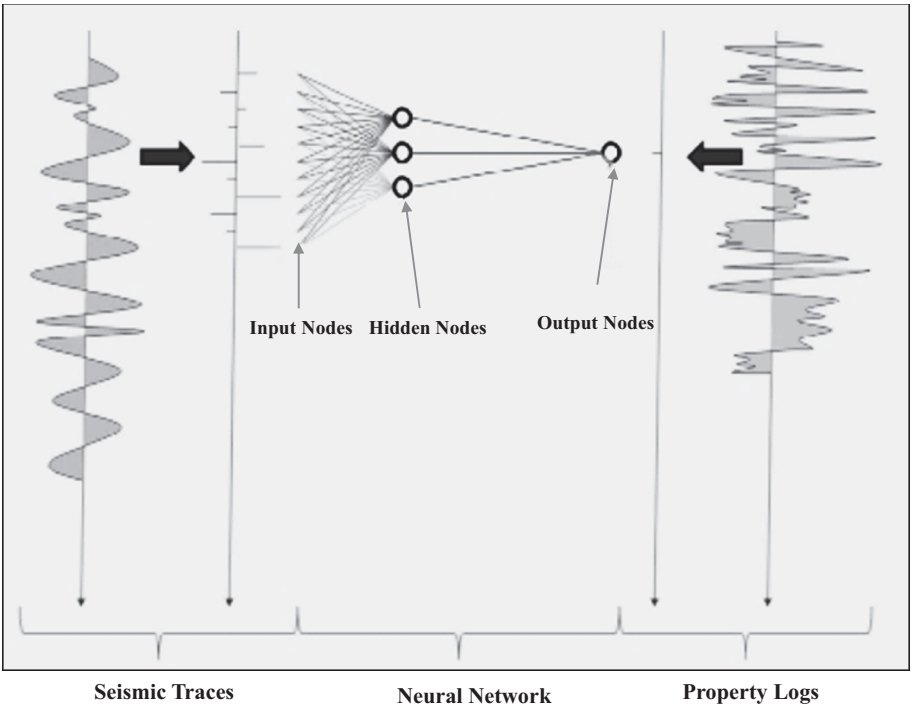

Fig. 8 Schematic approach of the link between seismic traces and property logs, through Neural Nets (Veeken et al. 2009)

The error is given by the function:

$$E = \frac{1}{n}\sum_{i=1}^{n}\left(L_i^{obs} - L_i^{cal}\right)^2, \tag{3}$$

where n is the number of observations, i denotes each observation, and L_i^{obs} and L_i^{cal} are the observed and calculated log responses, respectively.

Figure 8 shows the schematic approach of the link between seismic traces and property logs, through Neural Nets as followed by Veeken et al. (2009). Applying a GA during the learning phase of NN analysis reduces the risk for getting trapped in local minimum. Hampson et al. (2001) demonstrated that the more complex GI scheme generates improved results because it better honors certain subtle changes in the input data set.

In general the weights are applied either through gradient descendent method or through back propagation. In the present work initially 50 weight combinations are chosen at random and all are made to pass through the first iteration of the NN. The output is then compared with the observed datasets (i.e., well logs) by calculating the error function (Eq. 3). As soon as an error value is computed for each of the 50 input weight combinations the process enters into the genetic part of the algorithm (Klinger et al. 2008) with three operators: selection which equates to survival of the fittest; crossover which represents mating between individuals; and mutation which introduces random modifications

- *Selection operator*, it gives preference to better individuals, allowing them to pass on their genes to the next generation whose goodness of each individual depends on its fitness.

The fitness is determine through an objective function. This operator is in analogy to the natural selection hypothesis of Charles Darwin which favors only the best adapted individuals to survive. In the present study the survival criteria is given by the individual with the smallest error.

- *Crossover operator*, this operator is the prime distinguishing factor of GA from other optimization techniques. Two individuals are randomly chosen from the population using the selection operator and a crossover site along the bit strings. The values of the two strings are exchanged up to this point. The number of exchanged weights can be singular or multiple. The two new offspring created from this mating are put into the next generation of the population and by recombining portions of good individuals, this process is likely to create even better individuals. We have used single crossover point operator.
- *Mutation operator*, with some low probability, a portion of the new individuals will have some of their bits flipped. Its purpose is to maintain diversity within the population and inhibit premature convergence. Mutation alone induces a random walk through the search space. As in evolution single weights are exchanged randomly from one weight combination to another, i.e., single weight mutation operator is used. The operator adds a unit Gaussian distributed random value to the chosen gene.

It is important that a population has a constant number (e.g., 50) at each iteration of the inversion. Thus, even if selection reduces the size of the population by taking, for example, the 10 best weights, applying "cross-over" and "mutation" to those selected combinations of weights will recreate a full set of 50 "chromosomes" in the population.

The output of this workflow is a nonlinear multitrace operator which is applied to the whole seismic dataset, and transforms it into the property described by the logs used during the training phase (Klinger et al. 2008).

Seismic sub-cubes represent the operator structure (i.e., multitrace or 3D) and are utilized during the training and the modeling phase (Fig. 9). The middle trace passes through the well and the number of surrounding traces can be set from 0 to 10 in InLine and Xline directions. In the present case the inline and crossline half range is set to 1 and the vertical range is 15 ms. The program allows input of the top (K-IX Base) and bottom (K-X Top) surfaces between which the inversion is run. Computation of the derived neural NN operator is made step by step from top surface down to the bottom surface. Each step is equal to the seismic sample interval (e.g., 1–4 ms; Veeken et al. 2009).

In the present work relative acoustic impedance cube is generated from the seismic volume through volume attribute analysis. The relative acoustic impedance cube is trained with GR, LLD, NPHI and RHOB logs to establish a nonlinear correlation between acoustic impedance and petrophysical logs. The processing of GI setting is shown in Fig. 10. Using the above said GI approach, 3D attribute volume of the petrophysical property (in this case GR, LLD, NPHI and RHOB) are calculated. Advanced options allow definition of the "maximum number of iterations" and the desired "correlation threshold." The inversion stops once either of the above mentioned parameters is reached. "Nodes in hidden layer" is the neural net concept of describing the number of cells in the hidden layer used to compute the inversion operator. The "weight decay" is the NN smoother and overfitting prevention parameter. Hence, through a number of iteration, the process is repeated until a good match is observed between the actual and the synthetic logs. Figure 11 shows the comparison between the actual/synthetic logs generated from "Attribute based Inversion". In the present case, inversion of LLD log shows a better correlation compared to the other logs. Hence, LLD cube has been used further for Re classification. Finally, the calculated 3D attribute volume is re-sampled (up-scaled) in the structural grid.

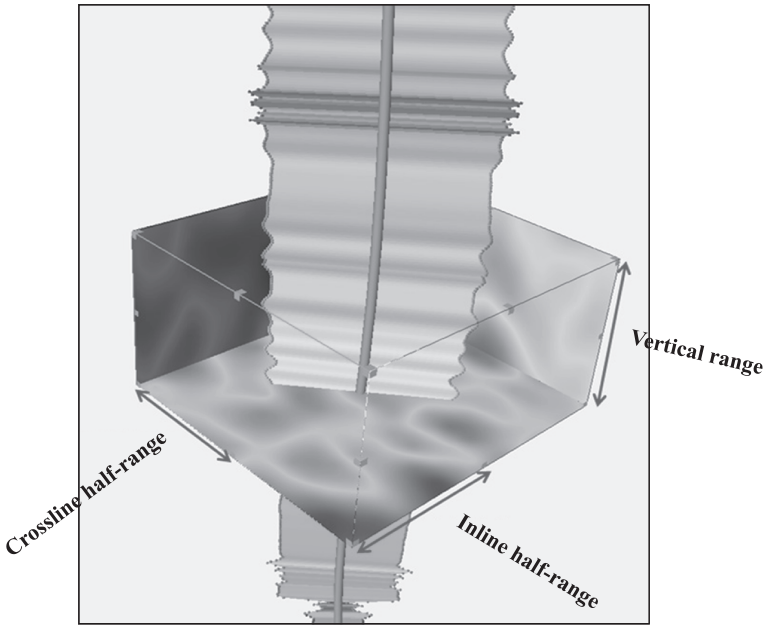

Fig. 9 Illustration of the sub cube used for the Neural network (Klinger et al. 2008)

3.7 Re/N-Re delineation

As the calculated and observed LLD curves (Fig. 11) show best correlation compared to the other logs, calculated LLD volume is preferred for seismo-facies volume calculation. In the present study following empirical relation is used for Re classification

```
if (LLD>K1)
        {
        Seismo-facies =1;
        }
else if  (LLD<K2)
        {
        Seismo-facies =2;
        }
else
        {
        Seismo-facies=0 ;
        }
```

(4)

where K_1 and K_2 are constant which depends on the average LLD observed in Re and N-Re zone, respectively. In this case we have choosen $K_1 = 4.5$ and $K_2 = 1.5$, as the average LLD value in G-Re and N-Re zone is around 4.5 and 1.5 ohm m, respectively in this field which may vary from field to field. The above calculation is important because, it effectively separates out the Re facies from the N-Re facies using the 3D log property calculated by ABI. For digitizing the seismo-facies model 0, 1 and 2 have been selected for the Re, G-Re and N-Re

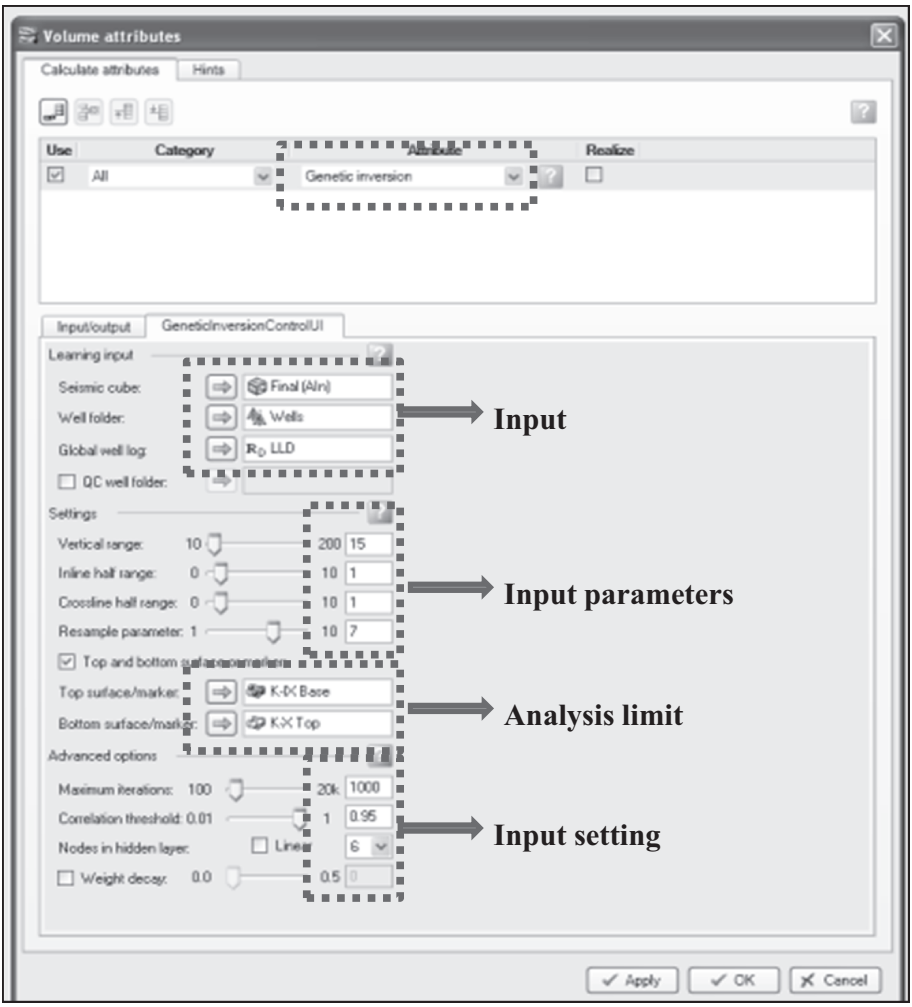

Fig. 10 The genetic inversion parameters setting (Petrel 2011.1)

facies, respectively. This means, it will model those grid having LLD $>$ 4.5 ohm m as G-Re by assigning a value 1. Similarly it will model those grid having LLD $<$ 1.5 ohm m as N-Re by assigning the value 2. Finally it will model the rest of the grid having LLD $<$ 4.5 ohm m and LLD $>$ 1.5 ohm m as Re by assigning the value 0. Hence, the field is broadly classified into three facies (Re, G-Re and N-Re).

3.8 Facies modeling

The quality of the Re has been further characterized by facies modeling. The Res are classified broadly into four facies: G-Re, M-Re, Re and N-Re. The facies log is upscaled using 'most of' (a geostatistical algorithm) within the structural grid. Facies modeling is processed by Sequential Indicator Simulation (a geostatistical algorithm) by considering the seismo-facies (Eq. 4) as the base model. The seismo-facies volume is used as a secondary input to provide

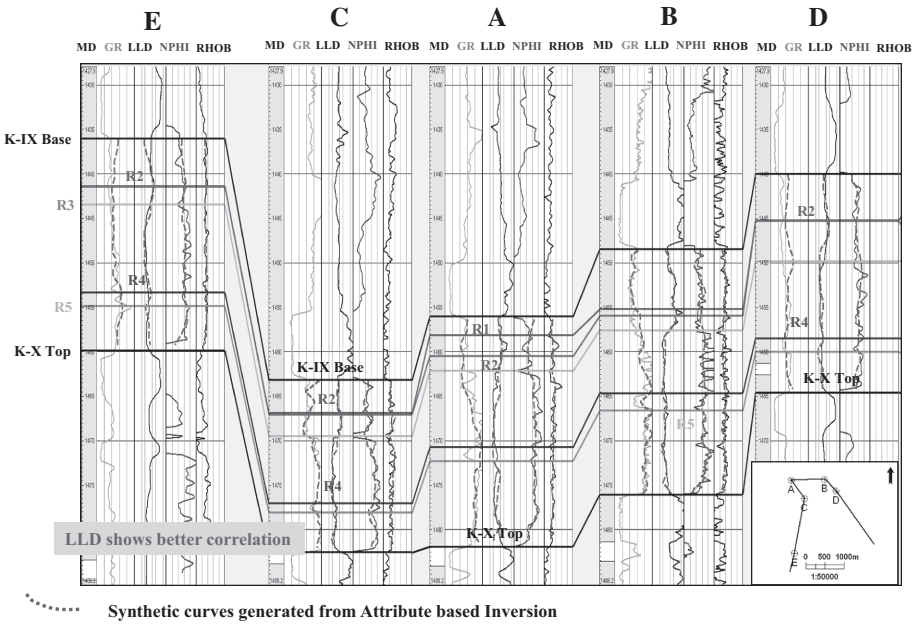

Fig. 11 Comparison with the actual/synthetic curves generated from "Attribute based Inversion". Inversion of LLD log shows a better correlation compared to the other logs

the trends to the facies modeling away from the well locations. This approach effectively uses the seismic property volume (or relative acoustic impedance volume) as a trend volume to characterize the G-Re, M-Re and Re and N-Re which is the major advantage of this approach over well based facies modeling. The intersectional and 3D view of facies distribution within the field is shown in Fig. 12. This shows that there exists a G-Re facies cluster in the N-W corner of the field.

3.9 PHI modeling

The PHI logs (calculated by Basic log analysis or Mineral modeling approach through available software in industry) are up scaled using 'most of' (a geostatistical algorithm) within the structural grid and distributed geo-statically by considering the facies model as the base model. Sequential Gaussian Simulation has been used for PHI modeling with the following constraints on the identified facies:

- PHI in N-Re ∼0 %,
- PHI in Re ∼8–12 %,
- PHI in M-Re ∼12–16 %,
- PHI in G-Re ∼16–20 %.

Figure 13 shows the intersectional and 3D view of PHI distribution within the field. This shows that G-Re facies cluster as obtained in Fig. 12 has good PHI.

3.10 Net–gross ratio modeling

Net–gross (N/G) ratio is calculated using the following empirical formula

$$\mathrm{N/G} = \mathrm{PHI}/\mathrm{PHI}_{\max}, \tag{5}$$

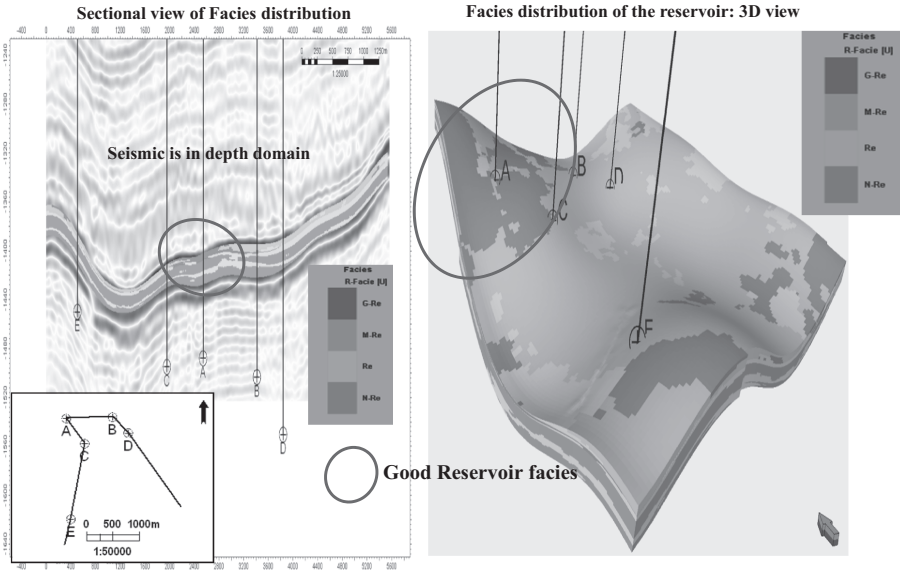

Fig. 12 Intersectional and 3D view of Facies model of the reservoir. The *highlighted part* represents the good reservoir facies cluster

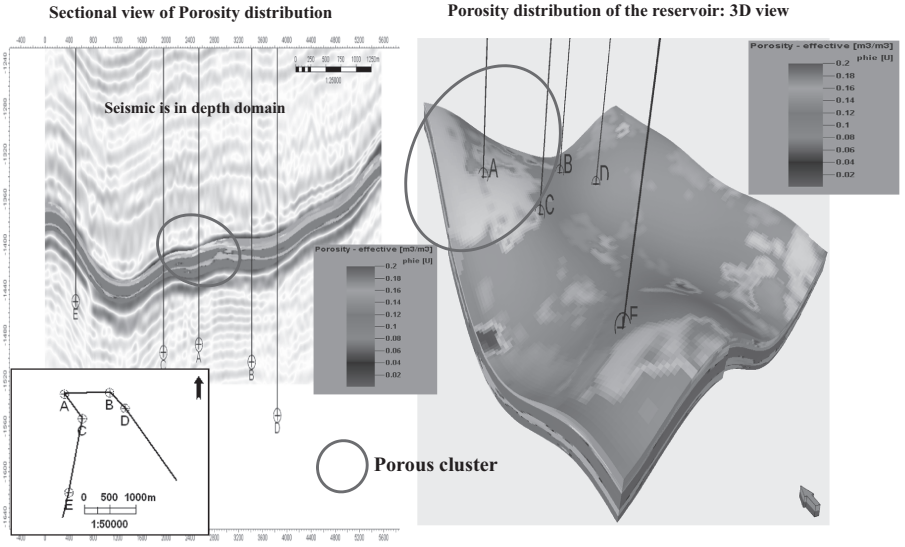

Fig. 13 Intersectional and 3D view of porosity model of the reservoir. The *highlighted part* represents good porous reservoir

where 'PHI_{max}' is the maximum PHI of the field and 'PHI' is the porosity value of individual grid. Equation 5 is one of standard relation used in industry for N/G calculation where N/G is highly depended on PHI. As N/G ratio is calculated from PHI, it shows a dependency on PHI

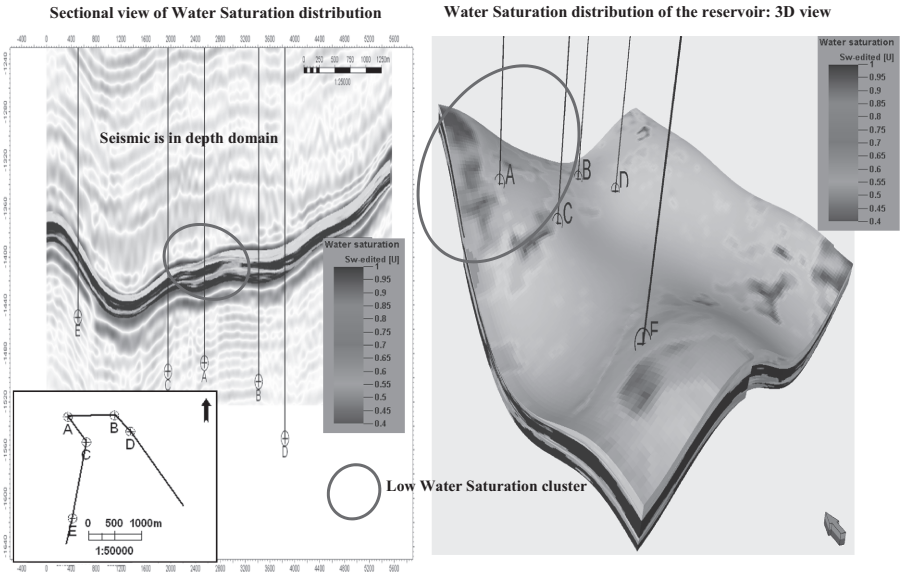

Fig. 14 Intersectional and 3D view of water saturation model of the reservoir. *Highlighted part* of the field has good oil saturation

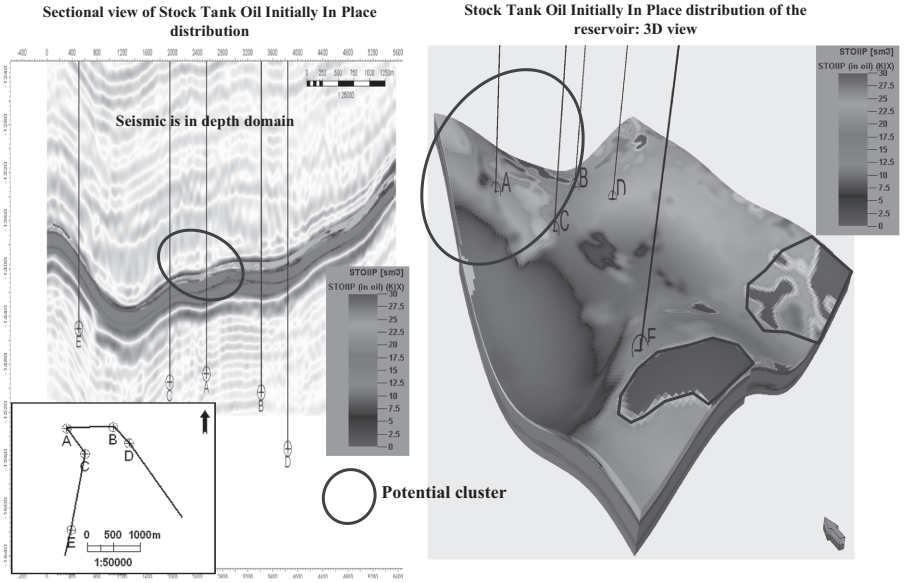

Fig. 15 Intersectional and 3D view of stock tank oil initially in place model of the reservoir. This figure shows that there exist a numbers of potential areas within the field. The *highlighted part* represents the potential areas

distribution and the model is similar to PHI model. The areas where the PHI is maximum N/G is assigned a value of 1, whereas, in other areas N/G is a fraction (less than 1) of actual PHI of the grid to the maximum PHI found in the field.

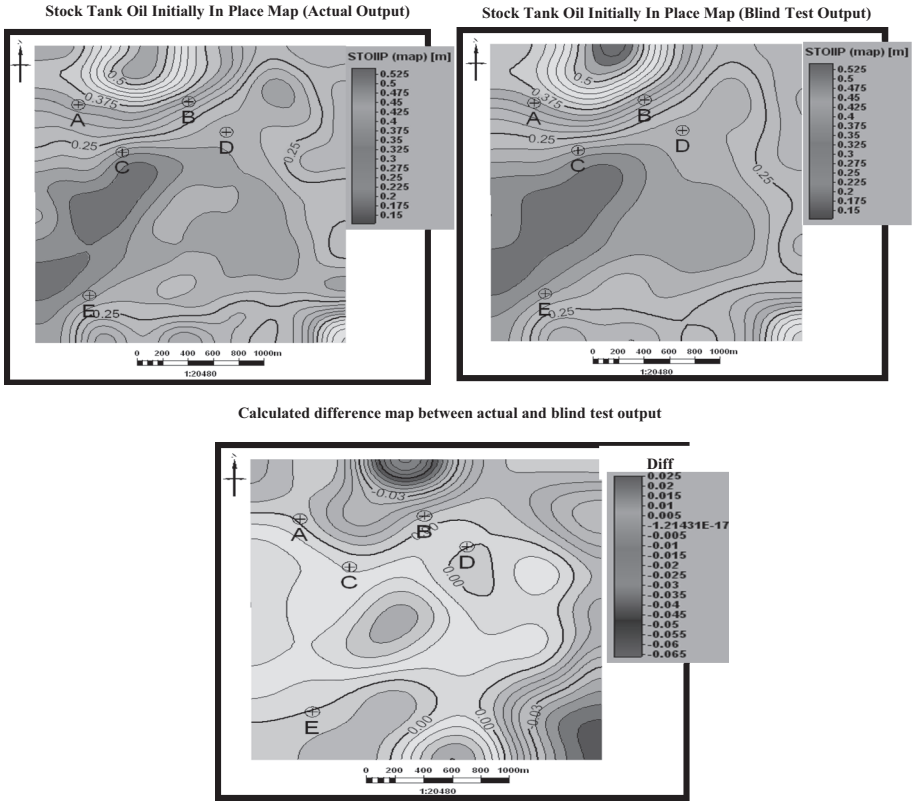

Fig. 16 Comparison of stock tank oil initially in place (STOIIP) map with blind test rest of the field area. The outputs of the blind test shows a similar results as obtained from the "Attribute based inversion" workflow

3.11 Sw modeling

Sw modeling is done in the similar way of PHI modeling. The Sw (calculated by Basic log analysis or Mineral modeling approach through available software in industry) logs are up-scaled and distributed geo-statistically taking facies model as base model. Following constraints were incorporated based on the identified facies:

- Sw in N-Re ∼100 %,
- Sw in Re ∼60–70 %,
- Sw in M-Re ∼50–60 %,
- Sw in G-Re ∼40–50 %.

Various representation of Sw distribution in the field is shown in Fig. 14. This shows that the highlighted part of the field has good oil saturation.

3.12 Volume calculation

Oil-in-place is also known as stock tank original oil-in-place (STOOIP) or stock tank oil-initially-in-place (STOIIP), referring to the oil in place before the commencement of production. Thus, it refers to the total oil content of an oil Re. As this quantity cannot be measured directly, it has to be estimated from other parameters measured prior to drilling or after pro-

duction has begun. Accurate estimation of stock tank oil and gas initially in place (STOIIP and GIIP) is one of the priority tasks before defining the reserves. We estimate STOIIP using grid base volume using inputs from PHI, Sw and N/G models. Oil volume expansion factor (B_o) value of 1.2 has been considered for volume estimation as per Standing correlation (1947). Various maps of STOIIP distribution in the field is shown in Fig. 15.

3.13 Blind test

To test the effectiveness of the "Attribute based inversion" technique the workflow has been repeated considering one of the wells (Well B) virtually absent in the field. Blind test is necessary where geostatistic is involved for modeling. The STOIIP modeling outputs of the blind test and "Attribute based inversion" technique is shown in Fig. 16 to compare the results. The outputs of the blind test shows a similar results as obtained from the "Attribute based inversion" workflow.

4 Conclusions

We have developed an ABI approach to differentiate the Res like sand/silts, silty sand or silty shale which was a challenging task earlier. The proposed approach is operative even if the Re is very thin (beyond seismic resolution) and can provide a way to generate 3D attribute volumes of log property from seismic and well log data. In addition, it is also effective in determining the Re geometry and quality of Re, which may help in planning future drilling locations. The efficiency of the proposed inversion scheme is demonstrated in the Kalol Field, Cambay Basin, India, where the oil recovery remained hardly around 10 % as it was a difficult task to identify the producing sequences within Kalol IX and Kalol X. The results shows that the proposed approach effectively resolve the Kalol Reservoir (2–5 m thick). The Re quality (G-Re or bad Re) geometry with areal extension of the Kalol Reservoir is delineated. Volumetric shows that there is still some potential remaining in the field. Suitably placing new wells it is quite possible to increase the productivity of the field. Hence, ABI should be applied on a routine basis as it helps to locate the areas of better reservoir facies in a field through seismic data greatly helps in improving the success rate, fluid recovery from the field and finally the economics of the investments.

Acknowledgments Authors are grateful to Prize Petroleum Company Limited (a wholly owned company of HPCL) and ONGC for providing the necessary information to carry out this work. Authors acknowledge their sincere thanks to Mr. M. K. Surana, CEO Prize Petroleum for giving permission to publish this work and moral support. Authors also acknowledge their sincere thanks to Mrs. Kavita Bhardwaj, Manager and Mr. Rejith M Rajan, Dy. Manager, Prize Petroleum for their valuable advices. Authors are grateful to Mr. Syam Sundar Yalamarty and Dr. Udayan Dasgupta Advisor Prize Petroleum for their valuable guidance.

References

Biswas SK (1987) Regional tectonic framework, structure and evolution of the western marginal basins of India. Tectonophysics 135:307–327

Biswas SK, Bhasin AL, Ram J (1993) Classification of Indian sedimentary basins in the framework of plate tectonics. Proc Second Semin Pet Basins India 1:1–46

Chatterjee CL, Bhardwaj A, Thakur RK, Chand R (2006) Delineation of Middle Eocene channel facies by synergistic approach—a case study from Wadu–Paliyad–North Kalol Field, Cambay Basin, India. In: 6th International conference and exposition on petroleum geophysics "Kolkata 2006"

Datta Gupta S, Farooqui MY, Ghosh UK (2010) Major pay sand delineation through inversion study from the mid to northern Cambay Basin Field. In: 8th Biennial international conference and exposition on petroleum geophysics, Hyderabad, India

Dhar PC, Bhattacharya SK (1993) Status of exploration in the Cambay basin. In: Biswas SK, Dave A, Garg P, Pandey J, Maithani A, Thomas NJ (eds) Proceedings second seminar on petroliferous basins of India, vol 2. Indian Petroleum Publishers, Dehra Dun, India, pp 1–32

Gorain S (2013) Integrated "Modified Inversion" approach to improve litho-facies mapping in clastic reservoirs in Kalol Reservoir, Cambay Basin. In: 10th International biennial inter-nation exposition. SPG, expanded abstracts, PID 36

Gorain S (2014) Multi-litho attribute based inversion for reservoir classification in Kalol Reservoir, Cambay Basin, India. J Indian Geophys Union 18(4):455–460

Gupta S, Chakraborty G, Kanungo US, Bharsakale A, Dattatraya K (2006) Reservoir delineation of lower Kalol pays and field growth in Wadu And Paliyad Areas, Cambay Basin, India. In: Geohorizones, January 2006

Hampson DP, Schuelke JS, Quirein JA (2001) Use of multiattribute transforms to predict log properties from seismic data. Geophysics 66:220–239

Jena AK (2008) Optimal recovery from low permeability reservoirs of Kalol Field, Cambay Basin, India—some key Issues. In: 7th Biennial international conference and exposition on petroleum geophysics. SPG, expanded abstracts, PID 180

Klinger J, Priezzhev I, Bo TH (2008) Petrel 2011.1 help manual. Schlumberger

Negi AS, Sahu SK, Thomas PD, Raju DSAN, Chand R, Ram J (2006) Fusing knowledge and seismic in searching for subtle hydrocarbon traps in India's Cambay Basin. Lead Edge 25(7):872–880

Standing MB (1947) A pressure–volume–temperature correlation for mixtures of California oil and gases. Drill Prod Pract API

Veeken P, Priezzhev I, Schmaryan L, Shteyn YI, Barkov AY, Ampilov YP (2009) Nonlinear multitrace genetic inversion applied on seismic data across the Shtokman field, offshore northern Russia. Geophysics 74(6):WCD49–WCD59